

# RECENT OBSERVATIONS, EXPERIMENTS AND SIMULATIONS OF ELECTRON CLOUD BUILDUP IN DRIFT SPACES AND QUADRUPOLE MAGNETS AT THE LOS ALAMOS PSR\*

Robert J. Macek<sup>#</sup>, Lawrence J. Rybarczyk, Andrew A. Browman, Rodney C. McCrady, and Thomas J. Zaugg, LANL, Los Alamos, NM 87544, U.S.A.

## Abstract

Recent beam studies have focused on improving our understanding of the role of quadrupole magnets as an important source of electron clouds (EC) which drive the observed e-p instability at the Los Alamos Proton Storage Ring (PSR). New experimental results making use of two longitudinal barriers to isolate the drift space electron diagnostic provide definitive evidence that most (~75%) of the drift space EC signal is "seeded" by electrons ejected longitudinally by ExB drifts from adjacent quadrupole magnets. This finding can explain why weak solenoids and TiN coatings in several drifts spaces had no effect on the e-p instability threshold.

## INTRODUCTION

Electron cloud (EC) generation in quadrupole magnets is hypothesized to play a key role in the e-p instability at the LANL PSR for several reasons. 1) The fluxes of seed electrons generated by proton beam losses are expected to be largest in quadrupoles because the beta functions and beam sizes are maximized there. This leads to grazing angle losses that produce large numbers of electrons per lost proton. In addition, we have no collimators to limit the beam halo produced by beam scattering in the stripper foil. 2) Analytical calculations and simulations of electron cloud generation in 3D quadrupoles at PSR [1] showed that a sizeable fraction of the electrons in the quadrupole are ejected longitudinally by ExB drifts with considerable energy, up to 2 keV or more, into the nearby drift spaces where the multipactor gain is considerably higher. 3) Electrons can be trapped radially in the mirror-like fields of the quadrupole. This can enhance the fraction of electrons that survive the passage of the gap between beam bunches.

To study the role of EC generation in quadrupoles and drift spaces and confirm the simulations, a low beam loss region of the PSR (section 4) has been instrumented with two special electron cloud diagnostics and two longitudinal electron barriers [2-4] as shown in the layout of Fig. 1. We designate the electron barriers "electron mirrors" since they reflect (when biased with negative voltage) electrons ejected from nearby quadrupoles and can be used to isolate the drift space diagnostic from electrons ejected from the quadrupoles. The drift space diagnostic is labeled ES41Y and the quadrupole diagnostic, labeled ES43Q, is located in the horizontally defocusing quadrupole at the downstream end of

section 4. Both of these diagnostics will measure the flux of electrons striking the chamber walls and, by pulsing the sweeping electrode near the end of the gap between bunch passages, can also measure the electrons surviving the gap. The studies reported here made use of the mirrors and two LANL adaptations of the RFA diagnostic [5] with a sweeping electrode added [2, 6].

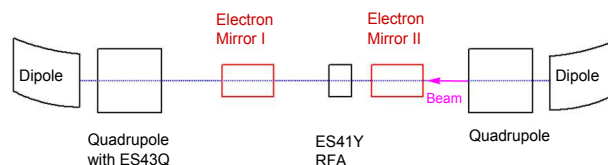


Figure 1: Layout of EC diagnostics in PSR section 4.

## RESULTS USING ELECTRON MIRRORS

The main features of experimental results using mirrors can be seen in a plot of several signals from an experiment where the mirrors and the ES41Y sweeper electrode were pulsed for several  $\mu\text{s}$  as shown in Fig. 2. The sweeper HV pulse was -500V and the mirrors pulsed at -2kV. There is a reflection in the HV monitor pulse for the sweeper that occurs because of imperfect attenuator in the return path. This can safely be ignored since it was not present on the pulse at the electrode.

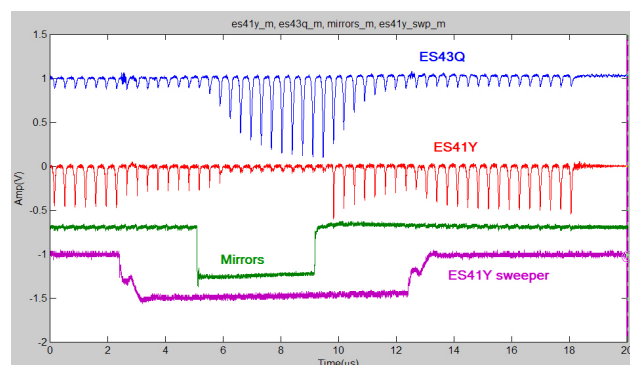


Figure 2: Simultaneous signal traces from an experiment where both the mirrors and the ES41Y (drift space) sweep electrode were pulsed for several  $\mu\text{s}$  (data taken 7/1/07, 5.8  $\mu\text{C}$  beam). Note that the electron detector responses appear at a somewhat later time due mostly to cable delays that have not been compensated for in this plot.

The ES41Y sweeper pulse clears the gap between bunches in the drift space and reduces the prompt signal ~30%. It is important to note that the prompt signal under these conditions is now only generated by multipacting on the present beam pulse and does not include a

\*Work supported by DOE SBIR Grant No. DE-FG02-04ER84105 and CRADA No. LA05C10535 between TechSource, Inc. and LANL.

<sup>#</sup>macek@lanl.gov

contribution from electrons captured at the end of the gap. When the mirrors are pulsed (-2kV) an additional large reduction (factor of ~4) is seen in the ES41Y prompt signal along with a growing signal in the quadrupole detector, ES43Q. The reduction is a result of preventing electrons ejected from the quadrupoles from reaching the space between the mirrors where the ES41Y diagnostic is located. The growing signal in ES43Q (quadrupole detector) that reaches a much larger equilibrium value is presumably the result of the Mirror I reflecting electron electrons ejected from the quadrupole back into the quadrupole where they can undergo additional amplification by trailing edge multipactor.

One problem with a long pulse on the ES41Y sweep electrode is that it can also affect the multipacting process. A better way to clear the gap is to pulse the sweeper electrode for a short time <100 ns during the gap passage. In this way the sweep field is absent during the beam pulse and will not affect the trailing edge multipactor. To do this we used a turn-by-turn sequence of 10 sweeper pulses timed toward the end of the gap as illustrated in Fig. 3.

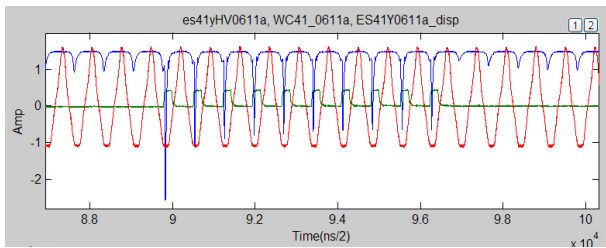


Figure 3: Signals for a turn-by-turn sequence of 10 ES41Y sweeper electrode pulses (green). The vertically displaced ES41Y signal with mirrors off (blue) is compared with the beam current signal (red) (data collected 6/11/08).

The first sweeper pulse clears out the gap and the subsequent prompt pulses are reduced since they are the result of multipactor amplification of seed electrons generated for just one turn. A comparison of the swept signals in Fig. 4 shows a factor ~5 reduction with the mirrors on (red) compared with the mirrors off (blue), which implies that ~80% of the swept signal is caused by electrons ejected from the nearby quadrupoles.

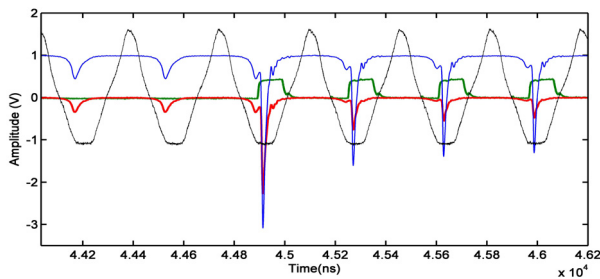


Figure 4: Signals for a turn-by-turn sequence of ES41Y sweeper electrode pulses (green). The ES41Y signal with mirrors on (red) is compared with mirror off (blue) and the beam current signal (gray).

A similar amplitude reduction occurs for the smaller prompt signals but is difficult to discern in Fig. 4 because

the display was adjusted to see the swept pulses. ES41Y signals at the end of the sequence are shown with better display gain in Fig. 5 for mirrors on and off. Here the first prompt signal after the last swept gap is down a factor of ~4 when the mirrors are on (red) compared to the situation when the mirrors are off (blue). This implies that a good fraction (~75%) of the prompt signal in the drift space diagnostic is also caused by electrons ejected from the nearby quadrupoles. Note that the prompt and swept pulses are starting to recover after the last sweeper pulse. Another plot showing the full recovery time for both signals is shown in Figure 6.

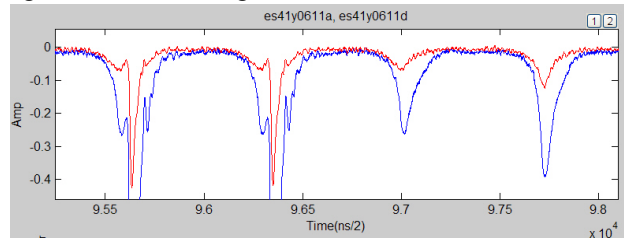


Figure 5: Signals near the end of the 10 turn sweep sequence comparing traces for mirrors off (blue) and mirrors on (red) DC at -2kV.

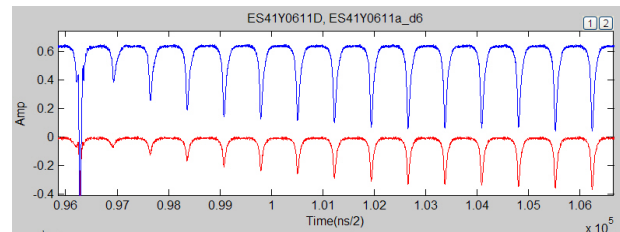


Figure 6: Signals in recovery after 10 turn sweep sequence comparing traces for mirrors off (blue) and mirrors on (red) DC at -2kV.

The recovery characteristics change somewhat with mirrors on compared to the case with mirrors off. In the former they recover to their equilibrium value in ~4 turns with a value of ~2.3 for the ratio of equilibrium pulse amplitude to that for the 1<sup>st</sup> pulse after the sweeping sequence. For the case with mirrors on, the recovery takes longer, ~8-9 turns, and the amplitude ratio is higher, ~5.4.

The large increase (factor of 5 to 10) in the ES43Q signal when the mirrors are pulsed also occurs when mirror I is biased continuously (DC) at -2kV. The effect has been seen experimentally many times whenever mirror I is biased more than -500V or so. The effect has not yet been adequately reproduced in simulations which are still a work in progress.

The results of the experiments with mirrors can help explain some longstanding puzzles such as the null effect of weak solenoids on the e-p instability threshold. Weak magnetic solenoids will suppress trailing edge multipacting, as was observed [7], but will not influence the electrons ejected from the quadrupoles during the beam pulse passage. These will move longitudinally in the drift space and oscillate transversely in the strong potential of the beam where they can still drive the instability. A similar argument holds for TiN, grooved

chambers, NEG coatings and other treatments that lower the SEY in drift spaces and thereby suppress multipacting. The electrons ejected from the quadrupoles are not affected by such measures in the drift spaces. To be effective for a long bunch machine the mitigation strategies must also be used to suppress EC buildup in the quadrupoles.

## SIMULATIONS

A program of simulations of these observations is underway using a modified version of the POSINST 12.1 code [8]. We have added several features which are better suited to the study of an extended longitudinal space including a linearized dipole end field, a static 3D numerical model of the ES41Y sweeper E (electric) field, a simplified longitudinal E field from the beam, longitudinal variation of seed electrons from beam losses, plus variation of beam sizes and EC space charge with  $z$  (longitudinal spatial coordinate along the beam direction).

Some inputs to the code are well determined such as beam sizes, beam intensity and the longitudinal profile of the beam. Other important inputs such as the peak secondary emission yield of the vacuum chambers and, in particular, the distributions and intensity of seed electrons from beam losses have large uncertainties. The hope is that we can vary a few selected parameters to simultaneously fit the results of several experiments. Another part of our strategy is to model beam loss details at PSR with the ORBIT code [9].

Recent simulations have provided additional insight into the ejection of electrons from a PSR quadrupole and the effect of the electron mirror. Fig. 7 shows a snap shot of electron  $Z$  and  $V_z$  coordinates on the trailing edge of the beam pulse taken from an animation. Electrons ejected from the downstream quadrupole are moving upstream of the quadrupole ( $-Z$  direction) and are reflected at the electron mirror. They are heading back towards the quadrupole where they can reenter the quadrupole and undergo additional multipactor amplification. An earlier version of the animation is available [10].

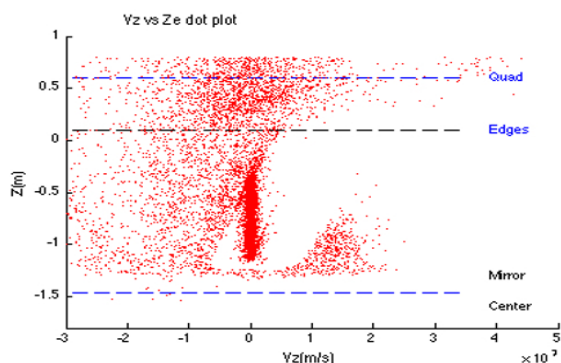


Figure 7: Snapshot of electron  $Z$  and  $V_z$  coordinates.

Recovery of the prompt signal amplitude after sweeping, as shown experimentally by the red trace (mirrors on) in Fig. 6, has been simulated for a 1 m drift space uniformly seeded by electrons from beam losses

well below ( $\sim 0.1\%$  of nominal) the average beam loss rate. A plot of the simulated signal is shown in Fig. 8 and reproduces the general features of the recovery data.

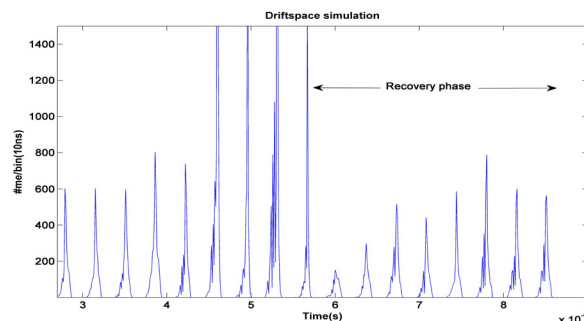


Figure 8: Simulation of the prompt signal recovery in ES41Y after a sweeping sequence of 4 pulses (produces the 4 off scale pulses). The prompt signals reached equilibrium (5 pulses shown) before the sweeper was pulsed.

## CONCLUSIONS

The experiments using electron mirrors convincingly demonstrate that  $\sim 75\%$  of the drift space prompt signal and swept signals are caused by electrons ejected from the nearby quadrupoles. This result, along with the insights from the simulations, can explain the null effect on the e-p instability of weak solenoids in selected drift spaces.

An effort is underway to improve the simulations for the main features of these experiments. A number of features such as an improved 3D model of the quadrupole field, mirrors, plus beam size and EC space charge variations with the longitudinal coordinate have been added to our modified version of the POSINST code. Detailed application of the augmented code is underway with some successes but is not yet completed.

## REFERENCES

- [1] R. J. Macek & M. T. Pivi, LANL report LA-UR-06-0179 (2005), also report LCC-0160 at [http://www-project.slac.stanford.edu/lc/ilc/TechNotes/LCCNotes/lcc\\_notes\\_index.htm](http://www-project.slac.stanford.edu/lc/ilc/TechNotes/LCCNotes/lcc_notes_index.htm).
- [2] R. Macek et al, PRSTAB **11**, 010101 (2008).
- [3] J. F. O'Hara et al, PAC07, p4117 (2007).
- [4] R. J. Macek et al, HB2008, talk WGA18 (2008).
- [5] R. A. Rosenberg and K. C. Harkay, Nucl. Instrum. Methods Phys. Res. **A453**, 507 (2000).
- [6] R. Macek et al, PAC03, p 508 (2003).
- [7] R. Macek, ELOUD'02, CERN-2002-001, p259.
- [8] M. T. F. Pivi & M. A. Furman, PRSTAB **6**, 034201 (2003).
- [9] J. D. Galambos, J. A. Holmes, and D. K. Olsen, ORBIT User Manual, Version 1.10, <http://neutrons.ornl.gov/APGroup/Codes/orbit.htm>.
- [10] HB2008 website, oral presentations only, Tues-WGA, 3Dqu\_Vz\_Zcor\_new\_axis3\_test20\_mir.avi.